Asociación Argentina de Mecánica Computacional

Mecánica Computacional Vol XXIX, págs. 3949-3976 (artículo completo)
Eduardo Dvorkin, Marcela Goldschmit, Mario Storti (Eds.)
Buenos Aires, Argentina, 15-18 Noviembre 2010

THE MOVING BOILING-BOUNDARY MODEL OF A VERTICAL TWO-PHASE FLOW CHANNEL REVISITED

Germán Theler[a,c], Alejandro Clausse[b] and Fabián J. Bonetto[c]

[a]*TECNA Estudios y Proyectos de Ingeniería S.A.*
Encarnación Ezcurra 365, C1107CLA Buenos Aires, Argentina

[b]*PLADEMA, CNEA-CONICET-Universidad Nacional del Centro*
Campus Universitario Paraje Arroyo Seco, B7000 Tandil, Argentina

[c]*Instituto Balseiro, CNEA-Universidad Nacional de Cuyo*
Av. Bustillo Km 9.5, R8400 Bariloche, Argentina

Keywords: Boiling, Channel, DAE, Two-phase

Abstract. Vertical flow involving phase changes is a subject of interest in several engineering branches, especially in the nuclear industry. Not only is there a concern about it in the design of boiling water reactors, but also safety evaluation and analysis in pressurised reactors involve a substantial amount of two phase flow calculations. As there is not yet a sound theoretical basis able to solve general problems, several mathematical models—often based on empirical or phenomenological observations—with limited applicability have been introduced to deal with particular situations. One example of these ad-hoc models is the moving boundary nodalisation proposed by Clausse and Lahey, that is reasonably simple and at the same time recovers experimental results with a high degree of accuracy. In this paper, the model is revisited and the equations are developed in detail keeping the intermediate mathematical steps. Alternative formulations that can be conveniently applied to different problems (i.e. single channel, parallel channels, adiabatic risers, non-steady external pressure drops, etc) are proposed, trying to take advantages of modern differential-algebraic equations solving methods. The general results obtained in this work can be extended to build particular models for different applications, including thermalhydraulic representations of nuclear power plants.

1 INTRODUCTION

The mathematical formulation of boiling two-phase flow presents several complexities and includes major nonlinear features that render a theoretical analysis very difficult. As an alternate approach, several models have been proposed to study flows involving phase changes. The moving boiling-boundary model of a vertical channel was first introduced by Clausse and Lahey in 1991 to provide a method to study the dynamics of boiling phenomena by using dynamical systems theory. The vertical boiling channel is a very convenient study case, since it has a simple formulation and yet exhibits most of the complex nonlinear features that are present in other problems. A review of the state-of-the-art classification of boiling instabilities was prepared by Kakac and Bon (2008). Some alternative ways of analysing the behaviour of a vertical boiling channel were introduced by Achard et al. (1985), Rizwan-Uddin and Dorning (1986), Clausse (1986), Guido Lavalle et al. (1991) and Delmastro et al. (2001).

The moving boiling-boundary model is interesting not only because of its ability to correctly represent a single vertical channel, but also because it can be extended to model other geometries and configurations that can be of particular interest for the industry. For example, using this model, Chang and Lahey (1997) developed a model of a boiling water reactor based on the moving boiling-boundary model. Theler (2008) studied the stability of the single vertical channel, but also added an adiabatic riser and studied parallel channels behaviour by computing fractal dimensions of asymptotic phase-space trajectories. He also developed models of nuclear power plants to analyse complex nonlinear behaviour and build stability maps.

In this work, we revisit the Clausse and Lahey model and derive it again from the basic conservation equations. We explain the rationale behind the assumptions and the decisions taken through the derivation, and explicitly show the intermediate mathematical steps used to arrive at the final equations. Written as a reference, this paper is intended to help the extension of the single channel model to other general cases where the basic assumptions do not hold (e.g. variable inlet enthalpy, nonuniform heating power, different geometries, etc). This way, one should be able to find the exact point of the derivation where a change should be introduced to extend the model and apply it to particular situations.

2 THE CONTINUOUS PROBLEM

The problem to be solved can be stated as follows. Given an uniformly heated vertical channel subject to constant pressure drop where subcooled fluid enters through the bottom and reaches the saturation conditions inside the channel (as depicted in figure 1), find the time-dependent fluid enthalpy, density and velocity profiles. The channel has an uniform cross section, and there are concentrated head losses at the channel inlet and outlet. A constant heating power is continuously applied through an ideal surface that has no heat capacity. Table 1 describes the nomenclature of the variables used throughout the mathematical development. Note that as the solution is based in a non-dimensional formulation, it is the actual dimensional variables that have a superscript.

2.1 Conservation equations

The proposed solution is based on the homogeneous equilibrium model and assumes that the following conditions hold:

- one-dimensional flux
- thermodynamic equilibrium between both phases

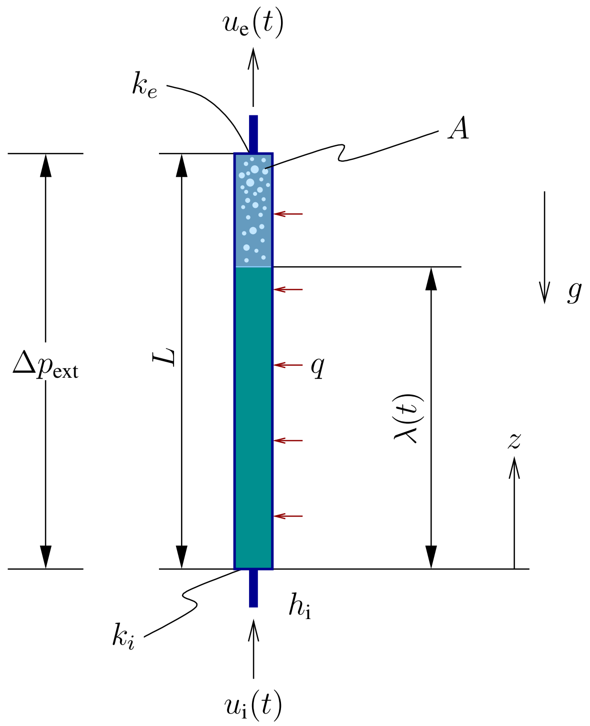

Figure 1: Vertical boiling channel of length L and cross section A subject to a fixed external pressure difference Δp_{ext}. A total power q is uniformly dissipated into the boiling fluid, that enters with a constant enthalpy h_i. There are concentrated head losses k_i and k_e at the channel inlet and outlet. In the transient case, both the inlet fluid velocity u_i and the boiling boundary λ may depend on time.

Variables	
t	time
z	axial coordinate
ρ	density
u	velocity
h	enthalpy
v	specific volume
q	total power
q''	heat flux
A	channel section
L	channel length
D	channel diameter
λ	boiling boundary
p	pressure
f	Darcy friction factor
k	concentrated head loss coefficient
g	gravity acceleration
δ	Dirac delta distribution

Subscripts	
ref	reference
ext	external
0	steady-state
H	hydraulic
f	saturated liquid
g	saturated vapour
fg	vapour-liquid difference
i	inlet
e	exit
Superscripts	
$+$	dimensional value

Table 1: Nomenclature used in the proposed solution

- no subcooled boiling
- constant pressure (i.e. $\Delta p^+_{\text{ext}} \ll p^+ \Rightarrow h^+_{fg}, v^+_{fg}$, etc. constants)
- constant inlet enthalpy
- negligible potential and kinetic energy changes

Under these assumptions, mass, energy and linear momentum conservation equations are, respectively

$$\frac{\partial}{\partial t^+}\Big(\rho^+\Big) + \frac{\partial}{\partial z^+}\Big(\rho^+ u^+\Big) = 0 \tag{1}$$

$$\frac{\partial}{\partial t^+}\Big(\rho^+ h^+\Big) + \frac{\partial}{\partial z^+}\Big(\rho^+ u^+ h^+\Big) = \frac{q^+}{A^+ L^+} \tag{2}$$

$$\frac{\partial}{\partial t^+}\Big(\rho^+ u^+\Big) + \frac{\partial}{\partial z^+}\Big(\rho^+ {u^+}^2\Big) = -\left(\frac{1}{2}\frac{f}{D_H^+} + \sum k_j \delta(z^+ - z_j^+)\right)\rho^+ {u^+}^2 - \rho^+ g^+ - \frac{\partial p^+}{\partial z^+} \tag{3}$$

where the positive z axis is in the upwards direction, with $z = 0$ at the channel inlet.

Besides, the thermodynamic equilibrium homogeneous model gives a fourth equation of state for the fluid

$$\rho^+ = \begin{cases} \rho_f^+ & \text{if } h^+ < h_f^+ \\ \dfrac{1}{v_l^+ + \dfrac{v_{fg}^+}{h_{fg}^+}\left(h^+ - h_f^+\right)} & \text{if } h^+ > h_f^+ \end{cases} \tag{4}$$

2.2 Non-dimensional equations

The problem and its solution can be better analysed—and by the way, its mathematical formulation simplified—by looking at the non-dimensional version of the equations. They can be obtained by diving each variable by a reference value, that is

$$\begin{aligned} t &= \frac{t^+}{t^+_{\text{ref}}} \\ z &= \frac{z^+}{z^+_{\text{ref}}} \\ \rho &= \frac{\rho^+}{\rho^+_{\text{ref}}} \\ u &= \frac{u^+}{u^+_{\text{ref}}} \\ h &= \frac{(h^+ - h_f^+)}{h^+_{\text{ref}}} \\ p &= \frac{p^+}{p^+_{\text{ref}}} \end{aligned}$$

These reference values can be, in principle, arbitrary. However, by choosing some convenient values one may arrive at a set of equations that depend on a minimal number of non-dimensional parameters, each one with a physical meaning. In the present solution, the proposed reference values are

$$\begin{aligned}
t_{\text{ref}} &= \nu^+ = \frac{\rho_f^+ A^+ L^+}{q^+}(h_f^+ - h_i^+) \\
z_{\text{ref}} &= L^+ \\
\rho_{\text{ref}} &= \rho_f^+ \\
u_{\text{ref}} &= \frac{L^+}{\nu} = \frac{q^+}{\rho_f^+ A^+ (h_f^+ - h_i^+)} \\
h_{\text{ref}} &= \frac{q^+}{\rho_f^+ A^+ u_0^+} \\
p_{\text{ref}} &= \rho_f^+ {u_{\text{ref}}^+}^2
\end{aligned}$$

The reference time ν^+ as defined is called *residence time* in the literature (Lahey and Moody, 1977). It refers to the time that a particle of subcooled fluid at the inlet conditions needs to reach the saturation enthalpy. In effect, consider a differential volume of fluid with density ρ^+ being heated by a volumetric source of intensity $q^+/(A^+L^+)$ resembling the problem conditions. In a differential time interval dt^+ the fluid would have increased its enthalpy by an amount dh^+ such that

$$\rho^+ \, dh^+ = \frac{q^+}{A^+L^+} \, dt^+$$

Solving for dt^+ and integrating both members, we have

$$\int_0^{\nu^+} dt^+ = \frac{A^+L^+}{q^+} \int_{h_i^+}^{h_f^+} \rho^+ dh^+$$

If we take the density ρ^+ as a constant, the equation for the residence time ν^+ follows.

The definition of the reference velocity as the quotient L^+/ν^+ implies that u_{ref}^+ is the inlet velocity that makes the fluid reach the saturation conditions exactly at the channel outlet. On the other hand, the velocity u_0^+ that appears in the reference enthalpy—in general different from u_{ref}^+—is the steady state value, i.e. the velocity that satisfies the steady momentum conservation equation. Note that h_{ref}^+ is the power to mass flow ratio at steady state, which is equivalent to the steady-state total enthalpy jump of the channel.

The dimensionless equation of state can be obtained dividing equation (4) by the fluid density. The dimensionless density of the subcooled liquid equals unity, and in the two-phase region:

$$\rho(h) = \frac{1}{1 + \dfrac{\rho_f^+ v_{fg}^+}{h_{fg}^+} h_{\text{ref}}^+ h} \qquad \text{if } h^+ > h_f^+$$

If we define the phase-change number—also known as the Zuber (1959) number—as

$$N_{\text{pch}} = \frac{h^+_{\text{ref}}}{h^+_{fg}} \frac{v^+_{fg}}{v^+_f} = \frac{q^+}{\rho^+_f A^+ u^+_0} \frac{v^+_{fg}}{h^+_{fg} v^+_f} \tag{5}$$

then we can write the dimensionless equation of state as

$$\rho = \begin{cases} 1 & \text{if } h \leq 0 \text{ (subcooled liquid)} \\ \dfrac{1}{1 + N_{\text{pch}}\, h} & \text{if } h > 0 \text{ (two-phase flow)} \end{cases} \tag{6}$$

We now turn our attention to the mass conservation equation (1) that can be nondimensionalised by using the dot rule for partial derivatives, as usual

$$\frac{\rho^+_f}{t^+_{\text{ref}}} \frac{\partial}{\partial t}\Big(\rho\Big) + \frac{\rho^+_f u^+_{\text{ref}}}{L^+} \frac{\partial}{\partial z}\Big(\rho u\Big) = 0$$

By noting that $t^+_{\text{ref}} = L^+/u^+_{\text{ref}}$, we derive

$$\frac{\partial}{\partial t}\Big(\rho\Big) + \frac{\partial}{\partial z}\Big(\rho u\Big) = 0 \tag{7}$$

In the same way, for the energy equation (2) we have

$$\begin{aligned} \frac{\rho^+_f h^+_{\text{ref}}}{t^+_{\text{ref}}} \frac{\partial}{\partial t}\Big(\rho h\Big) + \frac{\rho^+_f h^+_{\text{ref}} u^+_{\text{ref}}}{L^+} \frac{\partial}{\partial z}\Big(\rho u h\Big) &= \frac{q^+}{A^+ L^+} \\ \frac{\partial}{\partial t}\Big(\rho h\Big) + \frac{\partial}{\partial z}\Big(\rho u h\Big) &= \frac{q^+}{\rho^+_f A^+ u^+_{\text{ref}} h^+_{\text{ref}}} \\ \frac{\partial}{\partial t}\Big(\rho h\Big) + \frac{\partial}{\partial z}\Big(\rho u h\Big) &= \frac{u^+_0}{u^+_{\text{ref}}} \end{aligned}$$

It is useful to introduce at this point the subcooling number

$$N_{\text{sub}} = \frac{h^+_f - h^+_i}{h^+_{fg}} \cdot \frac{v^+_{fg}}{v^+_f} \tag{8}$$

that is proportional to the fluid subcooling at the channel inlet. Taking into account the definition of the chosen reference velocity, the quotient between the subcooling number and the phase-change number is

$$\frac{N_{\text{sub}}}{N_{\text{pch}}} = \frac{(h^+_f - h^+_i)\, v^+_{fg}}{h^+_{fg}\, v^+_f} \cdot \frac{\rho^+_f A^+ u^+_0\, h^+_{fg}\, v^+_f}{q^+\, v^+_{fg}} = \frac{u^+_0}{u^+_{\text{ref}}} \tag{9}$$

and the dimensionless energy equation may be written as

$$\frac{\partial}{\partial t}\Big(\rho h\Big) + \frac{\partial}{\partial z}\Big(\rho u h\Big) = \frac{N_{\text{sub}}}{N_{\text{pch}}} \tag{10}$$

Finally, the same procedure leads to the dimensionless linear-momentum equation

$$\frac{\partial}{\partial t}\Big(\rho u\Big) + \frac{\partial}{\partial z}\Big(\rho u^2\Big) = -\Big(\Lambda + \sum k_j \delta(z - z_j)\Big)\,\rho u^2 - \frac{\rho}{\mathrm{Fr}} - \frac{\partial p}{\partial z} \tag{11}$$

where we have introduced the distributed friction number

$$\Lambda = \frac{1}{2}\frac{f L^+}{D_H^+}$$

being f Darcy's friction factor, z_j the locations of the concentrated head losses

$$\Delta p_j^+ = k_j\, \rho^+ {u^+}^2 \tag{12}$$

and Fr the Froude number

$$\mathrm{Fr} = \frac{{u_{\mathrm{ref}}^+}^2}{g^+ L^+}$$

Although in general f depends only on the Reynolds number and the wall rugosity according to the Moody diagram for one-phase flow, we take it as a constant parameter. Thus, Λ is also a constant non-dimensional number. Moreover, in this paper we only allow concentrated head losses k_i and k_e only at the channel inlet and outlet.

It is useful to integrate the differential momentum conservation along the channel length

$$\frac{d}{dt}\left[\int_0^1 \rho u\, dz\right] + \left(\rho_e {u_e}^2 - \rho_i {u_i}^2\right) = -\Lambda \int_0^1 \rho u^2\, dz - \sum_j k_j\, \rho u^2 - \frac{1}{\mathrm{Fr}}\int_0^1 \rho\, dz + \mathrm{Eu} \tag{13}$$

where the last non-dimensional parameter, the Euler number

$$\mathrm{Eu} = \frac{\Delta p_{\mathrm{ext}}^+}{\rho_f^+\, {u_{\mathrm{ref}}^+}^2}$$

comes from the integral of the pressure gradient, that is equal to minus the external pressure difference. The conservation equations (7), (10) and (11) plus the equation of state (6) and the non-dimensional parameters that fully define the problem are summarised in table 2. The unknowns are $h(z,t)$, $\rho(z,t)$, $u(z,t)$ and $p(z,t)$.

2.3 Steady state

The model assumes constant properties of the fluid inside the channel, and we take the friction number Λ also as a constant. Thus, all the parameters listed in table 2 are constants. In the steady state all the time derivatives vanish. The single-phase length ranges from $z = 0$ up to $z = \lambda$, that is defined as the non-dimensional axial coordinate at which the fluid reaches the saturation conditions. In this zone, mass conservation gives $\rho(z) = 1$ and $u(z) = u_0^+/u_{\mathrm{ref}}^+$. Due to equation (9), the latter is given by

$$u(z) = \frac{N_{\mathrm{sub}}}{N_{\mathrm{pch}}} \qquad \text{if } z < \lambda \tag{14}$$

The steady-state energy equation for $z < \lambda$ gives

Dimensionless equations			
$$\frac{\partial \rho}{\partial t} + \frac{\partial(\rho u)}{\partial z} = 0$$			
$$\frac{\partial(\rho h)}{\partial t} + \frac{\partial(\rho u h)}{\partial z} = \frac{N_{\text{sub}}}{N_{\text{pch}}}$$			
$$\frac{\partial(\rho u)}{\partial t} + \frac{\partial(\rho u^2)}{\partial z} = -\Big[\Lambda + k_i \delta(z) + k_e \delta(z-1)\Big]\rho u^2 - \frac{\rho}{\text{Fr}} - \frac{\partial p}{\partial z}$$			
$$\rho = \begin{cases} 1 & \text{if } h \leq 0 \\ \dfrac{1}{1+N_{\text{pch}}\, h} & \text{if } h > 0 \end{cases}$$			
Dimensionless parameters			
N_{pch}	$=$	$\frac{q^+}{\rho_f^+ \, A^+ \, u_0^+} \frac{v_{fg}^+}{h_{fg}^+ v_f^+}$	Phase-change number
N_{sub}	$=$	$\frac{h_f^+ - h_i^+}{h_{fg}^+} \frac{v_{fg}^+}{v_f^+}$	Subcooling number
Fr	$=$	$\frac{{u_{\text{ref}}^+}^2}{g^+ L^+}$	Froude number
Eu	$=$	$\frac{\Delta p_{\text{ext}}^+}{\rho_f^+ \, {u_{\text{ref}}^+}^2}$	Euler number
Λ	$=$	$\frac{1}{2} \frac{f L^+}{D_H^+}$	Distributed friction number
k_i	$=$	$\frac{\Delta p_i^+}{\rho_i^+ {u_i^+}^2}$	Inlet head loss coefficient
k_e	$=$	$\frac{\Delta p_e^+}{\rho_e^+ {u_e^+}^2}$	Outlet head loss coefficient

Table 2: Dimensionless formulation of the vertical boiling channel problem

$$\frac{\partial(uh)}{\partial z} = \frac{N_{\text{sub}}}{N_{\text{pch}}}$$
$$\frac{\partial h}{\partial z} = 1$$

so, with the boundary condition $h(0) = h_i$ the enthalpy profile in the one-phase zone is

$$h(z) = h_i + z \qquad \text{if } z < \lambda \tag{15}$$

By definition, the non-dimensional inlet enthalpy is equal to

$$h_i = \frac{h_i^+ - h_f^+}{h_{\text{ref}}^+}$$

which can be rewritten taking into account the reference values and equation (9) as

$$h_i = -\frac{h_f^+ - h_i^+}{h_{\text{ref}}^+}$$
$$h_i = -\frac{q^+\nu^+}{\rho_f^+ A^+ L^+} \cdot \frac{\rho_f^+ A^+ u_0^+}{q^+}$$
$$h_i = -\frac{u_{\text{ref}}^+}{u_0^+}$$
$$h_i = -\frac{N_{\text{sub}}}{N_{\text{pch}}}$$

The boiling boundary λ is the axial coordinate at which $h(\lambda) = 0$, so from equation (15)

$$\lambda = -h_i$$
$$\lambda = \frac{N_{\text{sub}}}{N_{\text{pch}}} \tag{16}$$

and the enthalpy profile in the single-phase region is

$$h(z) = z - \frac{N_{\text{sub}}}{N_{\text{pch}}} \qquad \text{if } z < \lambda \tag{17}$$

In order for the fluid to boil inside the channel length, λ should be less than one or, equivalently, $N_{\text{pch}} > N_{\text{sub}}$. The subcooling number (8) depends only on the inlet conditions and is fixed directly by the pressure and inlet enthalpy. On the other hand, the phase-change number (5) depends, among others parameters, on the steady-state velocity u_0^+. Thus, N_{pch} indirectly depends on the rest of the parameters, including N_{sub} itself. Then, even though equation (16) seems simple, the difficulty of the problem resides in the computation of N_{pch} for a given set of dimensional parameters.

We now turn our attention to the energy equation in the two-phase zone. In the steady state,

$$\frac{\partial(\rho u h)}{\partial z} = \frac{N_{\text{sub}}}{N_{\text{pch}}} \tag{10}$$

From the equation of state (6) for the two-phase mixture, we have

$$\rho h = \frac{1-\rho}{N_{\text{pch}}}$$

and by replacing this product into equation (10)

$$\frac{\partial}{\partial z}\left(\frac{1-\rho}{N_{\text{pch}}}\cdot u\right) = \frac{N_{\text{sub}}}{N_{\text{pch}}}$$
$$\frac{\partial}{\partial z}\Big(u - \rho u\Big) = N_{\text{sub}}$$

By the continuity equation (7), in the steady state the spatial derivative of the product ρu vanishes. The result is that

$$\frac{\partial u}{\partial z} = N_{\text{sub}} \tag{18}$$

therefore the velocity profile in the two-phase zone is

$$\begin{aligned} u(z) &= u_0 + N_{\text{sub}}(z-\lambda) && \text{if } z > \lambda \\ u(z) &= \frac{N_{\text{sub}}}{N_{\text{pch}}} + N_{\text{sub}}\left(z - \frac{N_{\text{sub}}}{N_{\text{pch}}}\right) && \text{if } z > \lambda \\ u(z) &= N_{\text{sub}}\left(z - \frac{N_{\text{sub}}-1}{N_{\text{pch}}}\right) && \text{if } z > \lambda \end{aligned} \tag{19}$$

To simplify the math involved in obtaining the enthalpy profile $h(z)$ in the two-phase flow, we first define the dummy variable

$$\xi = z - \lambda$$

so ξ ranges between 0 and $1-\lambda$ in the two-phase zone. Then, going back once again to the steady-state energy equation

$$\frac{\partial(\rho u h)}{\partial \xi} = \frac{N_{\text{sub}}}{N_{\text{pch}}} \tag{20}$$

We now replace the velocity profile (19) and the equation of state (6) into equation (20)

$$\frac{\partial}{\partial \xi}\left[h(\xi)\,\frac{\frac{N_{\text{sub}}}{N_{\text{pch}}} + N_{\text{sub}}\,\xi}{1 + N_{\text{pch}}\,h(\xi)}\right] = \frac{N_{\text{sub}}}{N_{\text{pch}}}$$
$$\frac{\partial}{\partial \xi}\left[h(\xi)\frac{N_{\text{sub}}}{N_{\text{pch}}}\frac{1 + N_{\text{pch}}\,\xi}{1 + N_{\text{pch}}\,h(\xi)}\right] = \frac{N_{\text{sub}}}{N_{\text{pch}}}$$
$$\frac{\partial}{\partial \xi}\left[h(\xi)\frac{1 + N_{\text{pch}}\,\xi}{1 + N_{\text{pch}}\,h(\xi)}\right] = 1 \tag{21}$$

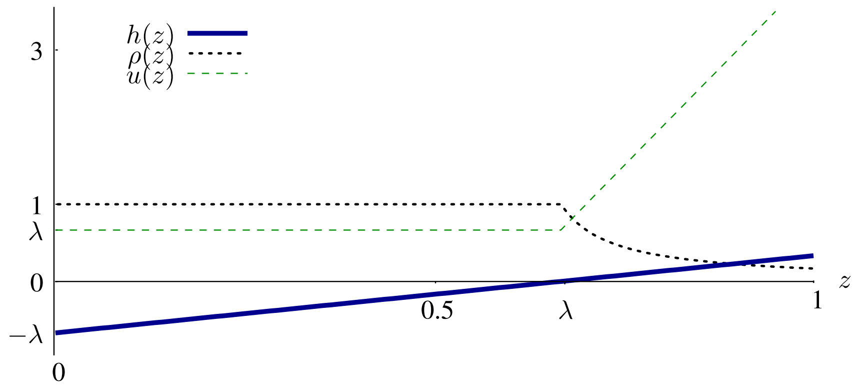

Figure 2: Steady-state dimensionless velocity, density and enthalpy profiles along the channel length for $N_{\text{pch}} = 15$ and $N_{\text{sub}} = 10$.

Equation (21) represents an ordinary differential equation with ξ as the independent variable that should be integrated to obtain the enthalpy profile $h(\xi)$. The boundary condition is

$$h(\xi = 0) = 0$$

by definition of the boiling boundary. Since the expression in brackets in equation (21) is continuous, the ordinary differential equation has an unique solution. It can be easily seen that this solution is

$$h(\xi) = \xi \quad \text{if } \xi > 0$$

By comparing this result with equation (17), we arrive at the conclusion that the non-dimensional enthalpy profile is linear with slope equal to one in the whole channel length

$$h(z) = z - \frac{N_{\text{sub}}}{N_{\text{pch}}} \tag{22}$$

With this result, the fluid density can be explicitly written as a function of the axial coordinate as

$$\rho(z) = \begin{cases} 1 & \text{if } z \leq \dfrac{N_{\text{sub}}}{N_{\text{pch}}} \\[2ex] \dfrac{1}{1 + N_{\text{pch}}\, z - N_{\text{sub}}} & \text{if } z > \dfrac{N_{\text{sub}}}{N_{\text{pch}}} \end{cases} \tag{23}$$

Combining equations (14) and (19), we obtain the velocity profile at steady state:

$$u(z) = \begin{cases} \dfrac{N_{\text{sub}}}{N_{\text{pch}}} & \text{if } z \leq \dfrac{N_{\text{sub}}}{N_{\text{pch}}} \\[2ex] N_{\text{sub}} \left(z - \dfrac{N_{\text{sub}} - 1}{N_{\text{pch}}} \right) & \text{if } z > \dfrac{N_{\text{sub}}}{N_{\text{pch}}} \end{cases} \tag{24}$$

Figure 2 shows the steady state profiles given by equations (22), (23) and (24). By fixing the subcooling and phase-change numbers, the velocity, enthalpy and density variations are automatically defined. Nevertheless, N_{pch} depends on the steady-state velocity u_0, which has been defined tautologically as the quotient between N_{sub} and N_{pch}. In order for the solutions in figure 2 to make sense, we must solve the momentum equation to obtain the phase-change number as a function of the problem parameters, namely the Euler and Froude numbers, the friction number Λ and the concentrated head losses coefficients k_i and k_e.

To compute the pressure drop as a function of z in the channel we must work with the continuous momentum equation (11). In the steady state and without concentrated head losses in the channel length, it reads

$$\frac{\partial(\rho u^2)}{\partial z} = -\Lambda\, \rho u^2 - \frac{\rho}{\text{Fr}} - \frac{\partial p}{\partial z}$$

For $z < \lambda$, the pressure gradient can be easily integrated

$$\begin{aligned}
\frac{\partial p}{\partial z} &= -\frac{\rho}{\text{Fr}} - \Lambda\, \rho u^2 - \frac{\partial(\rho u^2)}{\partial z} \\
\frac{\partial p}{\partial z} &= -\frac{1}{\text{Fr}} - \Lambda \left(\frac{N_{\text{sub}}}{N_{\text{pch}}}\right)^2 - \frac{\partial}{\partial z}\left[\left(\frac{N_{\text{sub}}}{N_{\text{pch}}}\right)^2\right] \\
\frac{\partial p}{\partial z} &= -\frac{1}{\text{Fr}} - \Lambda \left(\frac{N_{\text{sub}}}{N_{\text{pch}}}\right)^2 \\
p(z) &= p_i - \left[\frac{1}{\text{Fr}} - \Lambda \left(\frac{N_{\text{sub}}}{N_{\text{pch}}}\right)^2\right] z \qquad \text{if } z < \lambda
\end{aligned}$$

The expression for the two-phase zone is slightly more complicated

$$\begin{aligned}
\frac{\partial p}{\partial \xi} &= -\frac{\rho}{\text{Fr}} - \Lambda\, \rho u^2 - \frac{\partial(\rho u^2)}{\partial \xi} \\
\frac{\partial p}{\partial \xi} &= -\frac{1}{\text{Fr}}\left(\frac{1}{1+N_{\text{pch}}\,\xi}\right) - \Lambda\left[\left(\frac{N_{\text{pch}}}{N_{\text{sub}}} + N_{\text{sub}}\,\xi\right)^2\right] - \frac{\partial}{\partial \xi}\left[\left(\frac{N_{\text{pch}}}{N_{\text{sub}}} + N_{\text{sub}}\,\xi\right)^2\right] \\
\frac{\partial p}{\partial \xi} &= -\frac{1}{\text{Fr}}\left(\frac{1}{1+N_{\text{pch}}\,\xi}\right) - \Lambda\left[\left(\frac{N_{\text{pch}}}{N_{\text{sub}}} + N_{\text{sub}}\,\xi\right)^2\right] \\
&\qquad - \frac{2N_{\text{sub}}\left(\dfrac{N_{\text{pch}}}{N_{\text{sub}}} + N_{\text{sub}}\,\xi\right)}{1+N_{\text{pch}}\,\xi} + \frac{N_{\text{pch}}\left(\dfrac{N_{\text{pch}}}{N_{\text{sub}}} + N_{\text{sub}}\,\xi\right)^2}{(1+N_{\text{pch}}\,\xi)^2}
\end{aligned}$$

$$
\begin{aligned}
p(\xi) = -\Lambda \Bigg[& \frac{\left(N_{\text{pch}}^4 - 2\,N_{\text{pch}}^2\,N_{\text{sub}}^2 + N_{\text{pch}}^4\right)\,\log\left(N_{\text{pch}}\,\xi+1\right)}{N_{\text{pch}}^3\,N_{\text{sub}}^2} \\
& + \frac{N_{\text{pch}}\,N_{\text{sub}}^2\,\xi^2 + \left(4\,N_{\text{pch}}^2 - 2\,N_{\text{sub}}^2\right)\,\xi}{2\,N_{\text{pch}}^2}\Bigg] \\
& + N_{\text{pch}}\left[-\frac{\left(2\,N_{\text{sub}}^2 - 2\,N_{\text{pch}}^2\right)\,\log\left(N_{\text{pch}}\,\xi+1\right)}{N_{\text{pch}}^3} - \frac{N_{\text{sub}}^4 - 2\,N_{\text{pch}}^2\,N_{\text{sub}}^2 + N_{\text{pch}}^4}{N_{\text{pch}}^4\,N_{\text{sub}}^2\,\xi + N_{\text{pch}}^3\,N_{\text{sub}}^2} + \frac{N_{\text{sub}}^2\,\xi}{N_{\text{pch}}^2}\right] \\
& - 2\,N_{\text{sub}}\left(\frac{N_{\text{sub}}\,\xi}{N_{\text{pch}}} - \frac{\left(N_{\text{sub}}^2 - N_{\text{pch}}^2\right)\,\log\left(N_{\text{pch}}\,\xi+1\right)}{N_{\text{pch}}^2\,N_{\text{sub}}}\right) - \frac{\log\left(N_{\text{pch}}\,\xi+1\right)}{\text{Fr}\,N_{\text{pch}}}
\end{aligned}
$$

Nonetheless, the detailed pressure variation inside the channel is not needed to compute the phase-change number as a function of the other parameters. The integrated momentum equation (13) is enough. Replacing the the non-dimensional profiles obtained in figure 2 in it and now letting concentrated head losses both at the channel inlet and outlet, we get

$$
\begin{aligned}
\rho_e {u_e}^2 - \rho_i {u_i}^2 &= -\Lambda \int_0^1 \rho u^2\,dz - \sum_j k_j\,\rho u^2 - \frac{1}{\text{Fr}}\int_0^1 \rho\,dz + \text{Eu} \\
\frac{\left[u_0 + N_{\text{sub}}(1-\lambda)\right]^2}{1+N_{\text{pch}}(1-\lambda)} - {u_0}^2 &= -\Lambda \int_0^\lambda {u_0}^2\,dz - \Lambda \int_\lambda^1 \frac{\left[u_0 + N_{\text{sub}}(z-\lambda)\right]^2}{1+N_{\text{pch}}(z-\lambda)}\,dz \\
& \quad -k_i\,{u_0}^2 - k_e \frac{\left[u_0 + N_{\text{sub}}(1-\lambda)\right]^2}{1+N_{\text{pch}}(1-\lambda)} \\
& \quad -\frac{1}{\text{Fr}}\left[\int_0^\lambda dz + \int_\lambda^1 \frac{dz}{1+N_{\text{pch}}(z-\lambda)}\right] + \text{Eu}
\end{aligned}
$$

$$
\begin{aligned}
\frac{N_{\text{sub}}^2}{N_{\text{pch}}^2}\left(N_{\text{pch}} - N_{\text{sub}}\right) &= -\Lambda\frac{N_{\text{sub}}^3}{N_{\text{pch}}^3} - \Lambda\frac{N_{\text{sub}}^2}{N_{\text{pch}}^2}\left(1 - \frac{N_{\text{sub}}}{N_{\text{pch}}} + \frac{1}{2}N_{\text{pch}} - N_{\text{sub}} + \frac{1}{2}\frac{N_{\text{sub}}^2}{N_{\text{pch}}}\right) \\
& \quad -k_i\frac{N_{\text{sub}}^2}{N_{\text{pch}}^2} - k_e\frac{N_{\text{sub}}^2}{N_{\text{pch}}^2}\Big(1 + N_{\text{pch}} - N_{\text{sub}}\Big) \\
& \quad -\frac{1}{\text{Fr}}\frac{N_{\text{sub}}}{N_{\text{pch}}}\left[1 + \frac{\ln(1+N_{\text{pch}}-N_{\text{sub}})}{N_{\text{sub}}}\right] + \text{Eu}
\end{aligned}
$$

$$
\begin{aligned}
N_{\text{sub}}^2 N_{\text{pch}}\left(N_{\text{pch}} - N_{\text{sub}}\right) &= -\Lambda N_{\text{sub}}^3 - \Lambda N_{\text{sub}}^2 N_{\text{pch}}\left(1 - \frac{N_{\text{sub}}}{N_{\text{pch}}} + \frac{1}{2}N_{\text{pch}} - N_{\text{sub}} + \frac{1}{2}\frac{N_{\text{sub}}^2}{N_{\text{pch}}}\right) \\
& \quad -k_i N_{\text{sub}}^2 N_{\text{pch}} - k_e N_{\text{sub}}^2 N_{\text{pch}}\Big(1 + N_{\text{pch}} - N_{\text{sub}}\Big) \\
& \quad -\frac{N_{\text{sub}} N_{\text{pch}}^2}{\text{Fr}}\left[1 + \frac{\ln(1+N_{\text{pch}}-N_{\text{sub}})}{N_{\text{sub}}}\right] + \text{Eu}\cdot N_{\text{pch}}^3
\end{aligned}
$$

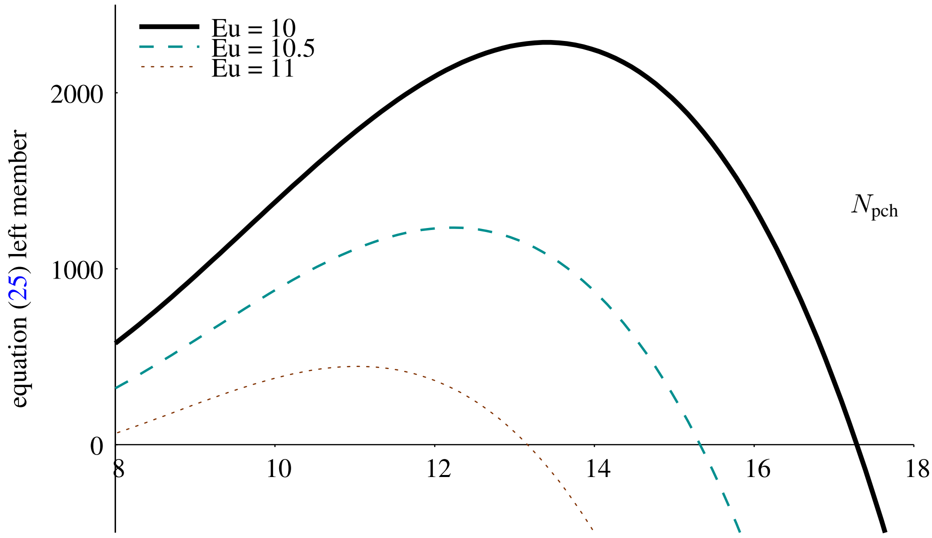

Figure 3: Left member of equation (25) as a function of the phase-change number for three different Euler numbers, with $N_{\text{sub}} = 8$, $\text{Fr} = 5$, $\Lambda = 3$, $k_i = 6$ and $k_e = 2$.

$$\begin{aligned} N_{\text{sub}}^2 N_{\text{pch}}^2 - N_{\text{sub}}^3 N_{\text{pch}} &= -\Lambda \left(N_{\text{sub}}^2 N_{\text{pch}} + \frac{1}{2} N_{\text{sub}}^2 N_{\text{pch}}^2 - N_{\text{sub}}^3 N_{\text{pch}} + \frac{1}{2} N_{\text{sub}}^4 \right) \\ &\quad - k_i N_{\text{sub}}^2 N_{\text{pch}} - k_e \left(N_{\text{sub}}^2 N_{\text{pch}} + N_{\text{sub}}^2 N_{\text{pch}}^2 - N_{\text{sub}}^3 N_{\text{pch}} \right) \\ &\quad - \frac{N_{\text{sub}} N_{\text{pch}}^2}{\text{Fr}} \left[1 + \frac{\ln(1 + N_{\text{pch}} - N_{\text{sub}})}{N_{\text{sub}}} \right] + \text{Eu}\, N_{\text{pch}}^3 \end{aligned}$$

This expression can be put as an implicit relationship between the phase-change number and the rest of the problem parameters

$$\begin{aligned} 0 = -N_{\text{pch}}^3 \cdot \text{Eu} + N_{\text{pch}}^2 &\left(N_{\text{sub}}^2 + \frac{1}{2} \Lambda N_{\text{sub}}^2 + k_e N_{\text{sub}}^2 \right) \\ &+ N_{\text{pch}} \left(-N_{\text{sub}}^3 + \Lambda N_{\text{sub}}^2 - \Lambda N_{\text{sub}}^3 + k_i N_{\text{sub}}^2 + k_e N_{\text{sub}}^2 - k_e N_{\text{sub}}^3 \right) \\ &+ N_{\text{pch}}^2 \frac{N_{\text{sub}}}{\text{Fr}} \left[1 + \frac{\ln(1 + N_{\text{pch}} - N_{\text{sub}})}{N_{\text{sub}}} \right] + \frac{1}{2} \Lambda N_{\text{sub}}^4 \end{aligned} \tag{25}$$

from where N_{pch} can be computed as a function of Eu, Fr, Λ, k_i, k_e and N_{sub}, that are directly known from the problem geometry and physical conditions.

To give an insight of what kind of relation equation (25) gives, figure 3 plots its left member as a function of N_{pch}. For a fixed set of parameters, the resulting phase-change number is the abscissa at which the plotted function crosses the zero axis. Note that only values of $N_{\text{pch}} > N_{\text{sub}}$ make sense, since otherwise there would be no two-phase flow at all and most of the equations derived in this section would not apply, including (25) itself.

Another approach that might be useful is to ask what external pressure difference, i.e. Euler number, would give a desired phase-change number. In this case, the solution has an explicit analytical expression

$$
\begin{aligned}
\mathrm{Eu} = {} & \frac{1}{N_{\text{pch}}}\left(N_{\text{sub}}^2 + \frac{1}{2}\Lambda N_{\text{sub}}^2 + k_e N_{\text{sub}}^2\right) \\
& + \frac{1}{N_{\text{pch}}^2}\Big(- N_{\text{sub}}^3 + \Lambda N_{\text{sub}}^2 - \Lambda N_{\text{sub}}^3 + k_i N_{\text{sub}}^2 + k_e N_{\text{sub}}^2 - k_e N_{\text{sub}}^3\Big) \\
& + \frac{N_{\text{sub}}}{N_{\text{pch}}}\frac{1}{\mathrm{Fr}}\left[1 + \frac{\ln(1 + N_{\text{pch}} - N_{\text{sub}})}{N_{\text{sub}}}\right] + \frac{1}{2}\frac{N_{\text{sub}}^4}{N_{\text{pch}}^3}\Lambda
\end{aligned} \tag{26}
$$

from where the required Euler number can be computed.

3 THE CLAUSSE-LAHEY MODEL

To numerically solve the time-dependant conservation equations we will revisit the model proposed by Clausse and Lahey based on the steady-state solution found in the preceding section. This model was first introduced in 1991 as an example of a two-phase flow nonlinear dynamical system with chaotic behaviour in a certain subset of the parameter space. The chaotic attractors found correspond to a vertical boiling channel with an adiabatic riser, model that is not discussed in this paper. Additional resources and related non-linear analysis theory is given by Lahey (1992).

The basic idea of the model is to convert the continuous equations into a set of differential and algebraic equations in an M-dimensional phase space by dividing the channel length in a finite number of cells and nodes. Then, the conservation equations are applied to each of them and some further assumptions are made in order to obtain a combination of algebraic and ordinary differential equations. With this ideas in mind, the model should consist of M equations of the form

$$
\mathbf{F}(\mathbf{x}, \dot{\mathbf{x}}) = 0 \tag{27}
$$

where $\mathbf{x} \in \mathbb{R}^M$ is the state vector of the problem.

Clausse and Lahey propose to divide the one-phase zone in N_1 cells, but with the particularity that their boundaries are allowed to move along the channel as time advances. Instead of computing the enthalpy at a given position, the model calculates the length at which a fixed enthalpy is reached by the fluid. As already shown, in the steady state the enthalpy varies linearly from $-N_{\text{pch}}/N_{\text{sub}}$ at the inlet, up to zero at $z = \lambda$. We define the position ℓ_n of the n-th single-phase node as the coordinate at which

$$
h(\ell_n) = h_n = \frac{N_{\text{sub}}}{N_{\text{pch}}}\left(\frac{n}{N_1} - 1\right) \tag{28}
$$

Garea (1998) shows that if N_1 is odd, the model has a mathematical pathology that is avoided by using an even number of nodes. In fact, experimental results are better resembled by using an even value for N_1, as shown by Garea et al. (1999).

A set of differential equations can be obtained for the positions of the nodes as a function of time by integrating the energy equation (10) between node n and $n+1$

$$
\int_{\ell_{n-1}}^{\ell_n} \frac{\partial(\rho h)}{\partial t}\, dz + \int_{\ell_{n-1}}^{\ell_n} \frac{\partial(\rho u h)}{\partial z}\, dz = \int_{\ell_{n-1}}^{\ell_n} \frac{N_{\text{sub}}}{N_{\text{pch}}}\, dz
$$

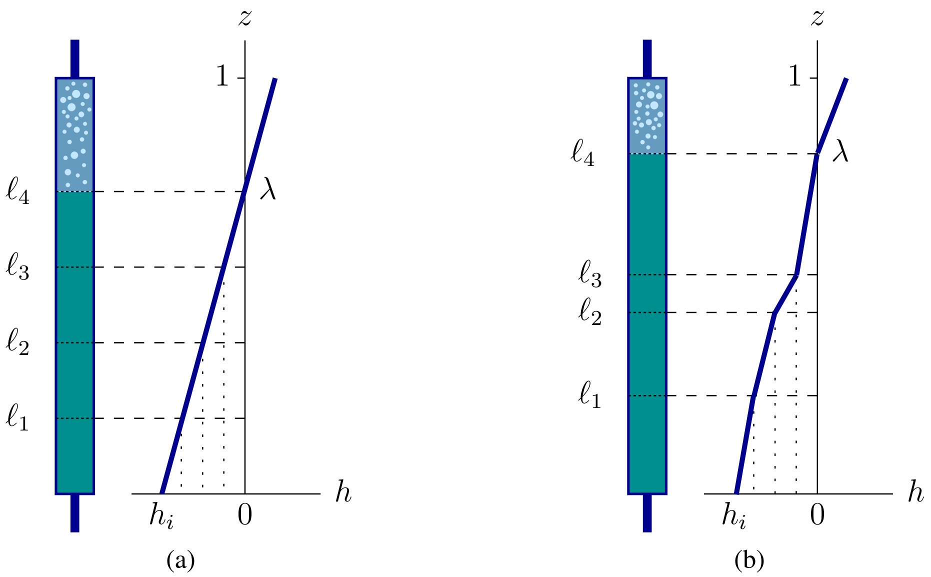

Figure 4: Basis of the moving boiling-boundary model. The one-phase zone is divided into $N_1 = 4$ cells whose boundaries are allowed to move following points of fixed enthalpy. (a) Node positions in the steady state. (b) Non-steady instantaneous state.

As the integration limits are time-dependant, to transform the partial derivative into a total derivative, the Leibnitz rule

$$\int_a^b \frac{\partial \mathcal{F}(x)}{\partial t}\, dx = \frac{d}{dt}\left[\int_a^b \mathcal{F}(x)\, dx\right] - \mathcal{F}(b)\frac{db}{dt} + \mathcal{F}(a)\frac{da}{dt}$$

must be used. Assuming that in the transient case the enthalpy between two adjacent nodes also varies linearly, and noting that for $z < \lambda$ it is $\rho(z,t) = 1$ and $u(z,t) = u_i(t)$ by mass conservation, we have

$$\frac{d}{dt}\left[\frac{(h_{n-1}+h_n)(\ell_{n-1}+\ell_n)}{2}\right] - h_n\frac{d\ell_n}{dt} + h_{n-1}\frac{d\ell_{n-1}}{dt} + u_i\cdot(h_n - h_{n-1}) = \frac{N_{\text{sub}}}{N_{\text{pch}}}(\ell_n - \ell_{n-1})$$

Taking into account equation (28) and rearranging terms, we obtain N_1 implicit equations for the position of the nodes as a function of the inlet velocity

$$\frac{1}{2}\left(\frac{d\ell_{n-1}}{dt} + \frac{d\ell_n}{dt}\right) + N_1(\ell_n - \ell_{n-1}) - u_i = 0 \tag{29}$$

where $\ell_0(t) = 0$. It is worth to note that the boiling boundary $\lambda(t)$ is equal to the last one-phase node position $\ell_{N_1}(t)$.

The original Clausse and Lahey model proposes to take the two-phase zone as a single node. Even though it may be analogously divided in a number of nodes (Chang and Lahey, 1997; Garea, 1998), the associated math gets quite complicated without a clear gain in accuracy.

Now, equations (29) depend on the inlet velocity. The main equation that involves u_i and from which a lot of information can be gained from is the integrated momentum equation (13)

$$\frac{d}{dt}\left[\int_0^1 \rho u\,dz\right] + \left(\rho_e {u_e}^2 - \rho_i {u_i}^2\right) = -\Lambda \int_0^1 \rho u^2\,dz - \sum_j k_j\,\rho u^2 - \frac{1}{\mathrm{Fr}}\int_0^1 \rho\,dz + \mathrm{Eu} \quad (30)$$

Before further working with this equation, we first derive a relationship between the inlet and the outlet velocities that allows us to evaluate the second term of equation (30). In the single-phase zone, mass conservation gives

$$u(z,t) = u_i(t) \qquad \text{if } z < \lambda(t)$$

Notably, in the two-phase zone, result (18) also holds in the transient case. In effect, the energy equation (10) says

$$\frac{\partial(\rho h)}{\partial t} + \frac{\partial(\rho u h)}{\partial z} = \frac{N_{\mathrm{sub}}}{N_{\mathrm{pch}}} \quad (10)$$

As in the steady-state case, from the equation of state (6)

$$\rho h = \frac{1-\rho}{N_{\mathrm{pch}}}$$

Replacing this product into equation (10)

$$\frac{\partial}{\partial t}\left(\frac{1-\rho}{N_{\mathrm{pch}}}\right) + \frac{\partial}{\partial z}\left(\frac{1-\rho}{N_{\mathrm{pch}}}\cdot u\right) = \frac{N_{\mathrm{sub}}}{N_{\mathrm{pch}}}$$

$$-\frac{\partial \rho}{\partial t} - \frac{\partial(\rho u)}{\partial z} + \frac{\partial u}{\partial z} = N_{\mathrm{sub}}$$

By the transient continuity equation, we obtain again equation (18)

$$\frac{\partial u}{\partial z} = N_{\mathrm{sub}} \quad (18)$$

that can be integrated in the interval $[\lambda, 1]$ with the condition $u(\lambda) = u_i$ to get

$$u_e(t) = u_i(t) + N_{\mathrm{sub}}\left[1 - \lambda(t)\right] \quad (31)$$

In the same way, an expression for the outlet density would help to evaluate the second term of the left member of equation (30). In the steady state we found that the enthalpy profile is linear along the whole channel. In the derivation of equations (29) we assumed a linear piecewise profile inside each cell defined by the moving nodes. We can suppose also a linear enthalpy profile in the two-phase zone with an arbitrary slope η that depends on time

$$h(z,t) = \eta(t)\cdot\left[z(t) - \lambda(t)\right] \qquad \text{if } z > \lambda \quad (32)$$

With this assumption, the density profile is

$$\rho(z,t) = \frac{1}{1 + N_{\mathrm{pch}}\,\eta[z - \lambda(t)]} \qquad \text{if } z > \lambda \quad (33)$$

and in particular, the exit density is

$$\rho_e(t) = \frac{1}{1 + N_{\text{pch}}\,\eta[1 - \lambda(t)]} \tag{34}$$

Looking at equation (30) once again, we now focus our attention on the Froude number term. The integral is equal to the total mass contained in the channel. Integrating the assumed density profile (33)

$$\begin{aligned}
m &= \int_0^1 \rho(z)\,dz \\
m &= \int_0^\lambda 1 \cdot dz + \int_\lambda^1 \frac{dz}{1 + N_{\text{pch}}\,\eta(z-\lambda)} \\
m &= \lambda + \frac{\ln\left[1 + N_{\text{pch}}\,\eta\,(1-\lambda)\right]}{N_{\text{pch}}\,\eta} \\
m &= \lambda + \frac{\ln\left(1/\rho_e\right)}{N_{\text{pch}}\,\eta}
\end{aligned} \tag{35}$$

If we wanted to into account the effects of single-phase compressibility to model for example natural circulation conditions, then the Boussinesq approximation would have to be used. It consists on assuming incompressibility of the fluid in every conservation equation except in the linear momentum equation term that represents the pressure difference due to the liquid weight. In this term—the one represented by equation (35) above—the single-phase density should be expanded up to the first order in a Taylor series as a function of the enthalpy. This characteristic is of particular importance in certain applications—for example natural circulation or chaotic regions—and is included in the original Clausse and Lahey (1991) model. However, this effect is neglected in the present work.

One further equation is needed because we do not know how to compute the slope η. We integrate the mass conservation equation (7) along the whole channel length

$$\begin{aligned}
\int_0^1 \frac{\partial \rho}{\partial t}\,dz + \int_0^1 \frac{\partial(\rho u)}{\partial z}\,dz = 0 \\
\frac{d}{dt}\int_0^1 \rho\,dz + \Big[\rho u\Big]_0^1 = 0
\end{aligned}$$

Noting that $\rho_i = 1$, we have the last equation we need to close our model

$$\frac{dm}{dt} + \rho_e u_e - u_i = 0 \tag{36}$$

We now have $N_1 + 5$ equations—(29), (30), (31), (34), (35) and (36)—for $N_1 + 5$ unknown variables, namely ℓ_1,...,ℓ_{N_1-1}, λ, u_i, u_e, ρ_e, m_e and η. The last step is to obtain the integrals that appear in the first term of each member of equation (30) as explicit expressions of the problem variables.

The first integral may be written as

$$\int_0^1 \rho u\, dz = u_i\lambda + \int_0^{1-\lambda} \frac{u_i + N_{\text{sub}}\xi}{1 + N_{\text{pch}}\,\eta\xi}\, d\xi$$
$$\int_0^1 \rho u\, dz = u_i\lambda + \frac{(u_i\,\eta N_{\text{pch}} - N_{\text{sub}})\ln\left[1+\eta N_{\text{pch}}(1-\lambda^+)\right] + \eta N_{\text{pch}} N_{\text{sub}}(1-\lambda^+)}{\eta^2 N_{\text{pch}}^2}$$
$$\int_0^1 \rho u\, dz = u_i\lambda + \frac{u_i \ln\left[1+\eta N_{\text{pch}}(1-\lambda)\right]}{\eta N_{\text{pch}}} - \frac{N_{\text{sub}}}{\eta N_{\text{pch}}}\left[\frac{\ln\left[1+\eta N_{\text{pch}}(1-\lambda)\right]}{\eta N_{\text{pch}}} + (1-\lambda)\right]$$

This expression can be simplified, by noting that from equation (35)

$$\frac{\ln\left[1 + N_{\text{pch}}\,\eta\,(1-\lambda)\right]}{N_{\text{pch}}\,\eta} = m - \lambda \tag{37}$$

so

$$\int_0^1 \rho u\, dz = u_i \cdot m + \frac{N_{\text{sub}}}{\eta N_{\text{pch}}}\Big(1 - m\Big) \tag{38}$$

and its total time derivative may be written as

$$\frac{d}{dt}\left[\int_0^1 \rho u\, dz\right] = m\cdot\frac{du_i}{dt} + u_i\cdot\frac{dm}{dt} - \frac{N_{\text{sub}}(1-m)}{\eta^2 N_{\text{pch}}}\cdot\frac{d\eta}{dt} - \frac{N_{\text{sub}}}{\eta N_{\text{pch}}}\cdot\frac{dm}{dt} \tag{39}$$

Analogously we can evaluate the integral that multiplies Λ in equation (30) as

$$\int_0^1 \rho u^2\, dz = \int_0^\lambda {u_i}^2\, dz + \int_0^{1-\lambda} \frac{(u_i + N_{\text{sub}}\xi)^2}{1 + N_{\text{pch}}\eta\xi}\, d\xi$$
$$\begin{aligned}\int_0^1 \rho u^2\, dz = {u_i}^2\lambda + \frac{1}{2(\eta N_{\text{pch}})^3}\Big[&2{u_i}^2(\eta N_{\text{pch}})^2 \ln[1+\eta N_{\text{pch}}(1-\lambda)] \\ &- 4u_i N_{\text{sub}}(\eta N_{\text{pch}})\ln[1+\eta N_{\text{pch}}(1-\lambda)] \\ &+ 2N_{\text{sub}}^2 \ln[1+\eta N_{\text{pch}}(1-\lambda)] + \lambda^2 N_{\text{sub}}^2(\eta N_{\text{pch}})^2 \\ &+ 2N_{\text{sub}}^2\lambda\left[\eta N_{\text{pch}} - (\eta N_{\text{pch}})^2\right] - 4N_{\text{sub}}u_i\lambda(\eta N_{\text{pch}})^2 \\ &+ 4N_{\text{sub}}u_i^+(\eta N_{\text{pch}})^2 + N_{\text{sub}}^2(\eta N_{\text{pch}})^2 - 2N_{\text{sub}}^2\eta N_{\text{pch}}\Big]\end{aligned}$$

In addition to the result of equation (37), we use (34) to write

$$\begin{aligned}\int_0^1 \rho u^2\, dz = m\cdot u_i^2 &+ \frac{2u_i N_{\text{sub}}\ln\rho_e}{(\eta N_{\text{pch}})^2} - \frac{N_{\text{sub}}^2 \ln\rho_e}{(\eta N_{\text{pch}})^3} + \frac{\lambda^2 N_{\text{sub}}^2}{2N_{\text{pch}}} + \frac{\lambda N_{\text{sub}}^2}{(\eta N_{\text{pch}})^2} - \frac{\lambda N_{\text{sub}}^2}{\eta N_{\text{pch}}} \\ &- \frac{2u_i\lambda N_{\text{sub}}}{\eta N_{\text{pch}}} + \frac{2u_i N_{\text{sub}}}{\eta N_{\text{pch}}} + \frac{N_{\text{sub}}^2}{2\eta N_{\text{pch}}} - \frac{N_{\text{sub}}^2}{(\eta N_{\text{pch}})^2}\end{aligned}$$
$$\begin{aligned}\int_0^1 \rho u^2\, dz = m\cdot u_i^2 &+ \frac{N_{\text{sub}}\ln(1/\rho_e)}{(\eta N_{\text{pch}})^2}\left(\frac{N_{\text{sub}}}{\eta N_{\text{pch}}} - 2u_i\right) + \frac{\lambda^2 N_{\text{sub}}^2}{2N_{\text{pch}}} + \frac{2u_i N_{\text{sub}}(1-\lambda)}{(\eta N_{\text{pch}})} \\ &+ \frac{N_{\text{sub}}^2}{\eta N_{\text{pch}}}\left[\left(\frac{1}{2} - \lambda\right) - \frac{1-\lambda}{\eta N_{\text{pch}}}\right]\end{aligned}$$

Thus, the integrated linear momentum equation (30) can be explicitly casted in terms of the problem variables and parameters as

$$
\begin{aligned}
m \cdot \frac{du_i}{dt} + u_i \cdot \frac{dm}{dt} - \frac{N_{\text{sub}}(1-m)}{\eta^2 N_{\text{pch}}} \cdot \frac{d\eta}{dt} - \frac{N_{\text{sub}}}{\eta N_{\text{pch}}} \cdot \frac{dm}{dt} + \rho_e {u_e}^2 - {u_i}^2 = \\
- \Lambda \left\{ m \cdot u_i^2 + \frac{N_{\text{sub}} \ln(1/\rho_e)}{(\eta N_{\text{pch}})^2} \left(\frac{N_{\text{sub}}}{\eta N_{\text{pch}}} - 2u_i \right) + \frac{\lambda^2 N_{\text{sub}}^2}{2 N_{\text{pch}}} + \frac{2u_i N_{\text{sub}}(1-\lambda)}{(\eta N_{\text{pch}})} \right. \\
\left. + \frac{N_{\text{sub}}^2}{\eta N_{\text{pch}}} \left[\left(\frac{1}{2} - \lambda \right) - \frac{1-\lambda}{\eta N_{\text{pch}}} \right] \right\} - k_i u_i^2 - k_e \rho_e u_e^2 - \frac{m}{\text{Fr}} + \text{Eu}
\end{aligned}
$$

To sum up, the moving boiling-boundary model of the two-phase vertical channel can be written as a set of $N_1 + 5$ differential-algebraic equations of the form (27). The resulting system is

$$
\begin{aligned}
0 &= \frac{1}{2} \left(\frac{d\ell_{n-1}}{dt} + \frac{d\ell_n}{dt} \right) + N_1(\ell_n - \ell_{n-1}) - u_i \qquad \text{for } n = 1, \ldots, N_1 \\
0 &= u_i - u_e + N_{\text{sub}} (1 - \lambda) \\
0 &= \rho_e - \frac{1}{1 + N_{\text{pch}}\, \eta (1-\lambda)} \\
0 &= \lambda - m + \frac{\ln (1/\rho_e)}{N_{\text{pch}}\, \eta} \\
0 &= \dot{m} + \rho_e u_e - u_i \\
0 &= m\, \dot{u}_i + u_i\, \dot{m} - \frac{N_{\text{sub}}(1-m)}{\eta^2 N_{\text{pch}}}\, \dot{\eta} - \frac{N_{\text{sub}}}{\eta N_{\text{pch}}}\, \dot{m} + \rho_e {u_e}^2 - {u_i}^2 + \frac{m}{\text{Fr}} - \text{Eu} \\
&\quad + \Lambda \left\{ m \cdot u_i^2 + \frac{N_{\text{sub}} \ln(1/\rho_e)}{(\eta N_{\text{pch}})^2} \left(\frac{N_{\text{sub}}}{\eta N_{\text{pch}}} - 2u_i \right) + \frac{\lambda^2 N_{\text{sub}}^2}{2 N_{\text{pch}}} + \frac{2u_i N_{\text{sub}}(1-\lambda)}{(\eta N_{\text{pch}})} \right. \\
&\quad \left. + \frac{N_{\text{sub}}^2}{\eta N_{\text{pch}}} \left[\left(\frac{1}{2} - \lambda \right) - \frac{1-\lambda}{\eta N_{\text{pch}}} \right] \right\} + k_i u_i^2 + k_e \rho_e u_e^2 \qquad (40)
\end{aligned}
$$

where $\ell_0 = 0$ and $\ell_{N_1} = \lambda$.

The basis of the moving boiling-boundary model can be used to extend the dynamical system (40) and apply it to industrial processes. In particular, the single vertical channel can be extended to model the primary circuit of nuclear power reactors. Theler (2008) discusses non-homogeneous and time-dependant power sources, inclusion of adiabatic risers and one-phase compressibility, non-constant inlet enthalpy and extensions for parallel channels. Chang and Lahey (1997) present a BWR mathematical model based on the moving nodes ideas, and Delmastro (1993) compare the results predicted by the model with actual two-phase flow experimental results.

3.1 The original Clausse-Lahey model

The system (40) is not the original form of the model proposed by Clausse and Lahey. The two-phase enthalpy slope η, introduced in the derivation proposed in section 3 to evaluate the density profile for $z > \lambda$ does not appear in the original formulation. It can be eliminated—and the phase-space dimension reduced—in several ways. We show one of them here by first noting from equations (34) and (35) that

$$\eta N_{\text{pch}} = \frac{1/\rho_e - 1}{1-\lambda}$$

and

$$\frac{(1-\lambda)\ln(1/\rho_e)}{1/\rho_e - 1} = m - \lambda \qquad (41)$$

With these results, we can write equation (38) as

$$\begin{aligned}\int_0^1 \rho u\, dz &= u_i \cdot m + \frac{N_{\text{sub}}}{\eta N_{\text{pch}}}\Big(1-m\Big) \\ &= u_i \cdot m + \frac{N_{\text{sub}}(1-\lambda)(1-m)}{1/\rho_e - 1}\end{aligned}$$

and its total time derivative

$$\begin{aligned}\frac{d}{dt}\int_0^1 \rho u\, dz = m\frac{du_i}{dt} + u_i\frac{dm}{dt} \\ + \frac{N_{\text{sub}}}{1/\rho_e - 1}\left[-(1-\lambda)\frac{dm}{dt} - (1-m)\frac{d\lambda}{dt} + \frac{(1-\lambda)(1-m)}{(1/\rho_e - 1)\rho_e^2}\frac{d\rho_e}{dt}\right]\end{aligned}$$

Furthermore, from equation (31)

$$N_{\text{sub}}(1-\lambda) = u_e - u_i$$

The individual terms of the distributed head loss can be rewritten as

$$\begin{aligned}\frac{N_{\text{sub}}\ln(1/\rho_e)}{(\eta N_{\text{pch}})^2}\left[\frac{N_{\text{sub}}}{\eta N_{\text{pch}}} - 2u_i\right] &= \frac{(1-\lambda)^2}{(1/\rho_e - 1)^2}N_{\text{sub}}\ln(1/\rho_e)\left[\frac{N_{\text{sub}}(1-\lambda)}{1/\rho_e - 1} - 2u_i\right] \\ &= \frac{(u_e - u_i)(m-\lambda)}{1/\rho_e - 1}\left[\frac{u_e - u_i}{1/\rho_e - 1} - 2u_i\right]\end{aligned}$$

$$\frac{2u_i N_{\text{sub}}(1-\lambda)}{\eta N_{\text{pch}}} = \frac{2u_i(u_e - u_i)(1-\lambda)}{1/\rho_e - 1}$$

$$\frac{N_{\text{sub}}^2}{\eta N_{\text{pch}}}\left[\left(\frac{1}{2} - \lambda\right) - \frac{1-\lambda}{\eta N_{\text{pch}}}\right] = \frac{N_{\text{sub}}(u_e - u_i)}{1/\rho_e - 1}\left[\left(\frac{1}{2} - \lambda\right) - \frac{(1-\lambda)^2}{1/\rho_e}\right]$$

and therefore

$$\int_0^1 \rho u^2\, dz = m \cdot u_i^2 + \frac{\lambda^2 N_{\text{sub}}^2}{2N_{\text{pch}}} + \frac{u_e - u_i}{1/\rho_e - 1}\left[(m-\lambda)\left(\frac{u_e - u_i}{1/\rho_e - 1} - 2u_i\right)\right.$$
$$\left. + N_{\text{sub}}\left(\frac{1}{2} - \lambda - \frac{(1-\lambda)^2}{1/\rho_e - 1}\right) + 2u_i(1-\lambda)\right]$$

Thus, a moving boiling-boundary model of dimension $N_1 + 4$ that does not depend explicitly on the slope η may be written as

$$
\begin{aligned}
0 &= \frac{1}{2}\left(\frac{d\ell_{n-1}}{dt} + \frac{d\ell_n}{dt}\right) + N_1(\ell_n - \ell_{n-1}) - u_i \qquad \text{for } n = 1, \dots, N_1 \\
0 &= u_i - u_e + N_{\text{sub}}\,(1-\lambda) \\
0 &= (1-\lambda)\frac{\ln(1/\rho_e)}{(1/\rho_e - 1)} - (m - \lambda) \\
0 &= \dot{m} + \rho_e u_e - u_i \\
0 &= m\,\dot{u}_i + u_i\,\dot{m} + \frac{N_{\text{sub}}}{1/\rho_e - 1}\left[-(1-\lambda)\,\dot{m} - (1-m)\,\dot{\lambda} + \frac{(1-\lambda)(1-m)}{(1/\rho_e - 1)\rho_e^2}\dot{\rho}_e\right] \\
&\quad + \rho_e {u_e}^2 - {u_i}^2 + \frac{m}{\text{Fr}} - \text{Eu} + k_i u_i^2 + k_e \rho_e u_e^2 \\
&\quad + \Lambda\left\{m\,u_i^2 + \frac{1}{2}\frac{N_{\text{sub}}^2}{N_{\text{pch}}}\lambda^2 + \frac{u_e - u_i}{1/\rho_e - 1}\left[(m-\lambda)\left(\frac{1-\lambda}{1/\rho_e - 1}N_{\text{sub}} - 2u_i\right)\right.\right. \\
&\quad \left.\left. + \lambda N_{\text{sub}}\left(\frac{1-\lambda}{1/\rho_e - 1} - 1\right) + N_{\text{sub}}\left(\frac{1}{2} - \frac{1-\lambda}{1/\rho_e - 1}\right) + 2u_i(1-\lambda)\right]\right\}
\end{aligned} \tag{42}
$$

that is equivalent to the original model introduced by Clausse and Lahey (1991). There are other similar forms of the model, as further discussed by Lahey (1992), Delmastro (1993) and Chang and Lahey (1997). It can be shown that systems (40) and (42) give the same results.

4 NUMERICAL RESULTS

In this section we give a brief survey of the results obtained by solving the moving boiling-boundary model. The set of DAE equations derived can be integrated in several different ways. In this work we use the dynamical system analysis code mochin, that is currently under development within a PhD thesis at Instituto Balseiro and is part of a suite of codes to aid in the analysis and design of power nuclear reactors (see Theler (2009) for a description of melon, a related control systems analysis software). This code reads a text input file where a DAE system is defined, integrates the equations by interfacing with the SUNDIALS library and then outputs the results as specified by the user in the input file. Appendix A shows the basic input file used in the generation of the figures discussed in this section.

Figure 5 shows the generation of a self-sustained oscillation. Starting from a phase-space position near the fixed point defined by the steady-state conditions, the inlet velocity oscillates with a growing amplitude up to a certain level, in which the motion sets down into a periodic pattern. This self-sustained mass flow oscillations were observed experimentally by Delmastro (1993), and it can be seen that the Clausse and Lahey model is able to reproduce them. The

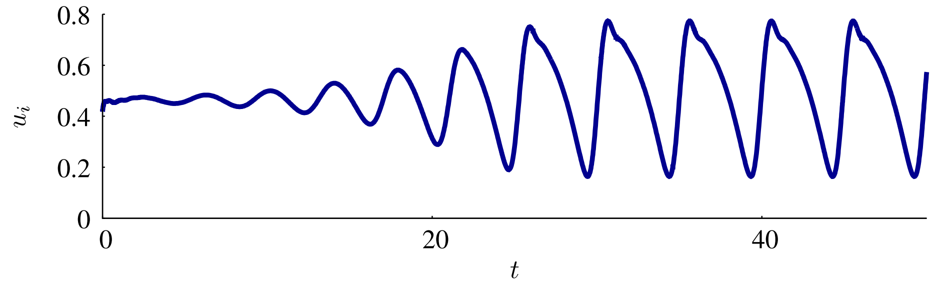

Figure 5: Inlet velocity u_i vs time for a transient that starts with a perturbation on u_i and leads to a self sustained oscillation. The non-dimensional parameters used were $N_{\text{pch}} = 14$, $N_{\text{sub}} = 6.5$, $\text{Fr} = 1$, $\Lambda = 3$, $k_i = 6$, $k_e = 2$, $\text{Eu} = 9.4987\dots$ (according to equation (26)).

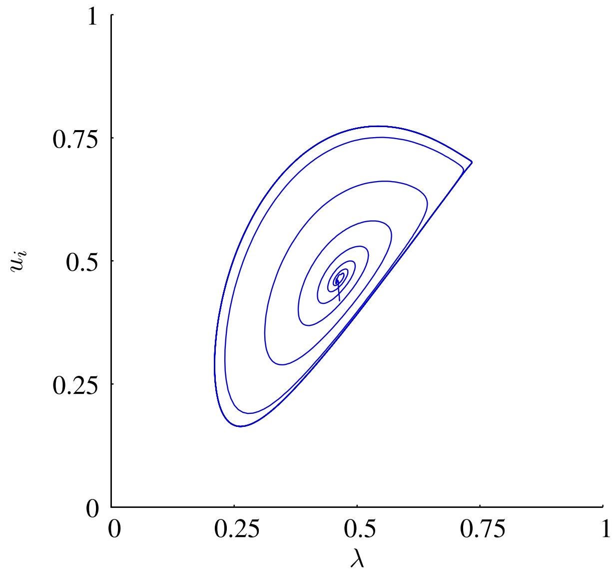

Figure 6: Phase-space portrait projection on plane u_i vs. λ of the time sequence represented in figure 5. The trajectory starts with $u_i(0) = 0.9N_{\text{sub}}/N_{\text{pch}}$ and evolves into a limit cycle.

same result may be displayed in another way, as shown by figure 6 where a projection of the $(N_1 + 5)$-dimensional phase space over the u_i-λ plane can be seen. For the selected parameters, the steady-state phase-space point is not stable, so it repels nearby trajectories. However, a stable limit cycle exists that attracts the solution and sets the trajectory into a periodic motion.

The fixed-point stability depends on all the dimensionless parameters. Nevertheless, the two most important are the phase-change number and the subcooling number. In effect, with a slight change in N_{pch}, the channel behaves in quite different forms. Figure 7 shows two trajectories corresponding to a stable fixed point and to a unstable fixed point with no stable limit cycle. In the first case, the fixed point attracts the green orbit and in the other one, not only is the trajectory repelled away from the fixed point, but also since there exists no stable limit cycle, the inlet velocity inverts its sign and the model no longer holds.

With this idea in mind, and taking advantage of mochin's capabilities to carry on parametric studies, a rough N_{sub} vs. N_{pch} stability map can be quickly constructed. Figure 8 shows with a colour legend the final integration time for 384,000 individual simulations, each for a different

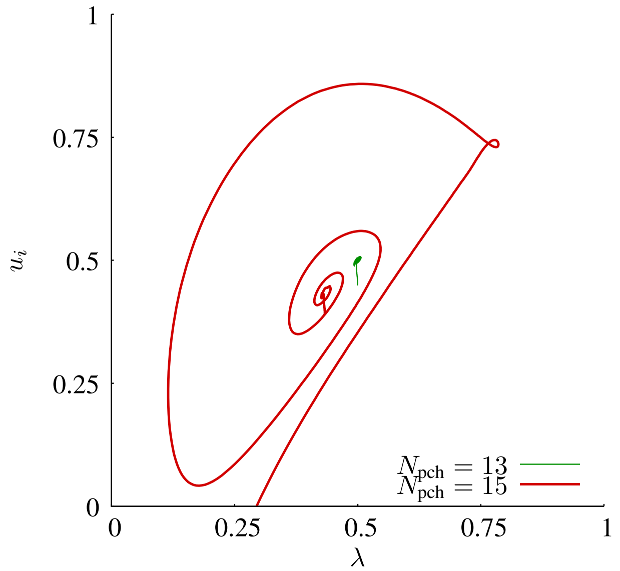

Figure 7: Phase-space portrait projection on plane u_i vs. λ for two cases that differ slightly in the phase-change number, with the rest of the non-dimensional parameters as in figure 5. In each case, the perturbation starts with $u_i(0) = 0.9N_{\text{sub}}/N_{\text{pch}}$. For $N_{\text{pch}} = 13$, the trajectory is attracted by the fixed point $u_i = \lambda = N_{\text{sub}}/N_{\text{pch}} = 0.5$. For $N_{\text{pch}} = 15$, there are oscillations that grow in amplitude and even the flow direction is inverted. When the state vector leaves the plotted square the mathematical model no longer holds.

combination of N_{sub} and N_{pch}. The desired non-dimensional final integration time was set to 50. As the input file tests u_i and λ to be always greater than zero and less than one or otherwise the integration ends, if the actual end time is less than 50, then the proposed combination results in an unstable case. On the other hand, as the solver has an adaptive step integration method, if the solution reaches a steady state then the derivatives will be small and the time step will increase. Thus, chances are that the integration will not end exactly at the desired en time but at a time somewhat greater than 50. Finally, if a limit cycle is reached, then the time step will tend to remain small and the final integration time will be almost equal to 50. It should be said that these is a very rough method, as this reasoning may lead us to think that there are stable limit cycles for parameters that we know cannot have periodic motion. This is the case of the Ledinegg instability zone, where the colour yellow appears because the trajectories are still inside the $[0, 1]$ interval for $t < 50$ but they would leave it if the integration time was larger. More complex and accurate instability analysis should be done to obtain sound conclusions. See for example Theler (2008) where the fractal dimension of the asymptotic trajectories is studied to analyse the stability of several cases. Nevertheless, preliminary maps like the one shown in figure 8 can help to check and correct errors when starting to work in a problem. Its construction took less than twenty minutes in an i7 processor with eight cores.

5 CONCLUSIONS

The moving boiling-boundary model for a vertical two-phase flow channel was revisited and its equations were derived from scratch showing explicitly most of the intermediate mathematical steps that lead to the final formulation. Starting from the conservation equations, the steady-state continuous profiles where found. Then, the Clausse and Lahey basic idea of mov-

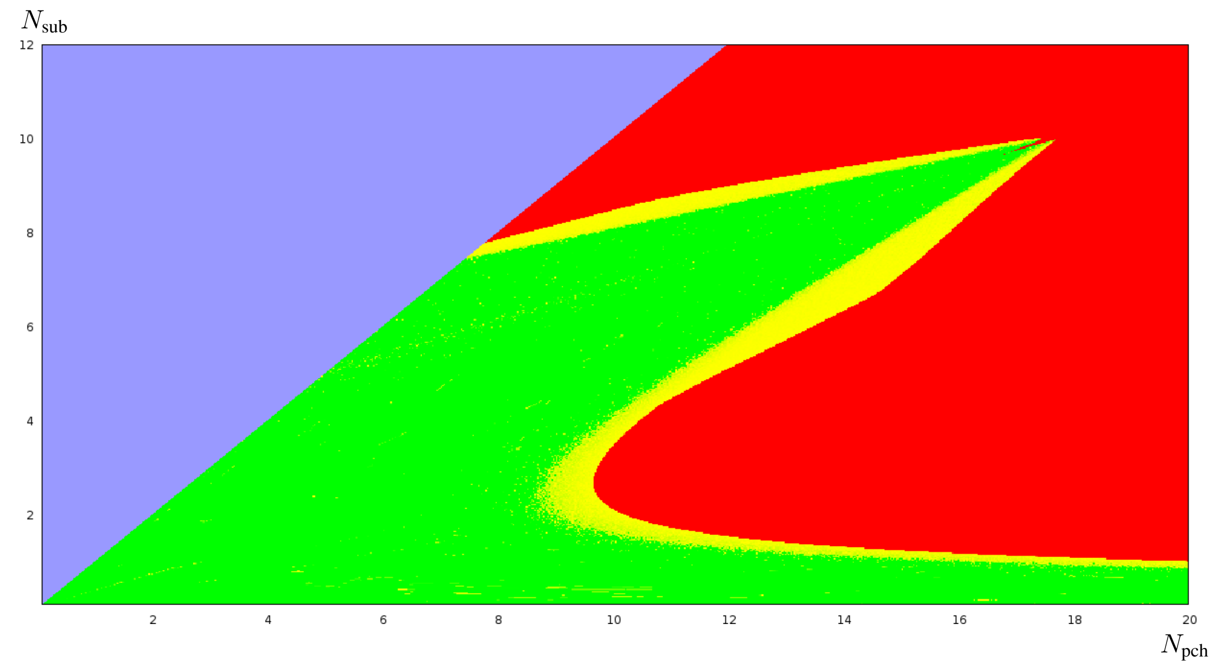

Figure 8: Preliminary N_{sub} vs. N_{pch} stability map constructed by means of a parametric study on the moving boiling-boundary model. Green points may correspond to stable cases, yellow to limit cycles and red to unstable orbits that leave the $[0, 1]$ interval. For $N_{\text{pch}} < N_{\text{sub}}$ (blue zone), the fluid does not boil and the model does not hold.

ing nodes was applied and an implicit system of differential-algebraic equations was obtained. If the single-phase zone is divided into N_1 cells, a first approach gives a system of dimension $N_1 + 5$ that with a proper mathematical manipulation can be reduced to $N_1 + 4$, matching the original formulation.

By having a detailed mathematical derivation of the model, the single channel case can be extended to handle more general problems, that is the main objective of this paper. Moreover, the form of the resulting equations is well suited to be solved with modern DAE integrator libraries. Thus, this combination provides convenient way to simulate and analyse two-phase boiling problems of interest for the industry.

REFERENCES

Achard J., Drew D., and Lahey R.T. The analysis of nonlinear densitiy-wave oscillations in boiling channels. *Journal of Fluid Mechanics*, 155, 1985.

Chang C. and Lahey R.T. Analysis of chaotic instabilities in boiling systems. *Nuclear Engineering and Design*, 167, 1997.

Clausse A. *Efectos no lineales en inestabilidades de ondas de densidad en flujo de dos fases*. Tesis de Doctorado en Ingeniería Nuclear, Instituto Balseiro, 1986.

Clausse A. and Lahey R.T. The analysis of periodic and strange attractors during density-wave oscillations in boiling flow. *Chaos, Solitons and Fractals*, 1(2), 1991.

Delmastro D. *Aplicación de la teoría de sistemas dinámicos al análisis de inestabilidades termohidráulicas*. Ph.D. thesis, Instituto Balseiro, 1993.

Delmastro D., Juanicó L., and Clausse A. A delay theory for boiling flow stability analysis. *International Journal of Multiphase Flow*, 27, 2001.

Garea V. *Nodal analysis of two-phase flow instabilities*. Ph.D. thesis, Rensselaer Polytechnic Institute, 1998.

Garea V., Drew D., and Lahey R.T. A moving-boundary nodal model for the analysis of the stability of boiling channels. *International Journal of Heat and Mass Transfer*, 42:3575–3584, 1999.

Guido Lavalle G., Converti J., and Clausse A. Density-wave oscillations in parallel channels—an analytical approach. *Nuclear Engineering and Design*, 125, 1991.

Kakac S. and Bon B. A review of two-phase flow dynamic instabilities in tube boiling systems. *International Journal of Heat and Mass Transfer*, 51, 2008.

Lahey R.T., editor. *Boiling Heat Transfer: Modern Developments and Advances*. Elsevier, 1992.

Lahey R.T. and Moody F.J. *The thermal hydraulics of a boiling water nuclear reactor*. Monograph series on nuclear science and technology. American Nuclear Society, 1977.

Rizwan-Uddin and Dorning J.J. Some nonlinear dynamics of a heated channel. *Nuclear Engineering and Design*, 93, 1986.

Theler G. *Non-linear analysis of instabilities in the coupled thermal hydraulic-neutronic problem*. Master's Thesis, Instituto Balseiro, 2008.

Theler G. Simulación de experimentos de estabilidad en flujo de dos fases acoplando RELAP a un código externo de control inteligente basado en lógica difusa. *Mecánica Computacional*, XXVIII:3169–3183, 2009.

Zuber N. Hydrodynamic aspects of boiling heat transfer. Technical Report AECU 4439, US AEC, 1959.

A SAMPLE MOCHIN INPUT FILE

Figures from section 4 were constructed with the dynamical system analysis code mochin, part of the wasora suite under development for a PhD thesis in Nuclear Engineering at Instituto Balseiro. This code reads an input file that should define a system of implicit DAEs and then, it integrates them by using the SUNDIALS library. An example input from which figure 5 and 6 were constructed is the following file:

```
##############################
# vertical boiling channel
# clausse & lahey nodalization, nondimensional DAE version
# version with eta (N_1+5 variables) as presented at MECOM 2010
# 17-Aug-2010
# gtheler@tecna.com
##############################

##############################
# phase-space definition
##############################
N_1 = 6       # nodes in the single-phase region

# should N_1 change, please change the
# variables that span the phase space
DAE_PHASE_SPACE l_1, l_2, l_3, l_4, l_5, l_6, u_i, rho_e, u_e, m, eta

# the boiling boundary is equal to the last one-phase node position
# and we refer to it as lambda throughout the file
ALIAS lambda l_6

##############################
# non-dimensional parameters
##############################
```

```
N_pch = 14     # phase-change number
N_sub = 6.5    # subcooling number

Fr = 1         # froude number
Lambda = 3     # distributed friction number
k_i = 6        # inlet head loss coefficient
k_e = 2        # outlet head loss coefficient

# compute the needed euler (external pressure) number
Eu = {  (1/N_pch)*(N_sub^2 + 0.5*Lambda*N_sub^2 + k_e*N_sub^2)
      + (1/N_pch^2)*(-N_sub^3 + Lambda*N_sub^2 - Lambda*N_sub^3
                     + k_i*N_sub^2 + k_e*N_sub^2 - k_e*N_sub^3)
      + (N_sub/N_pch)* 1/Fr * (1 + log(1 + N_pch - N_sub)/N_sub)
      + 0.5*N_sub^4/N_pch^3*Lambda }

# declare the above parameters and steady-state values
# as constants so they are not computed each time step
CONST N_pch N_sub Fr Eu b Lambda k_i k_e
CONST u_i_star lambda_star m_star rho_e_star u_e_star eta_star


##############################
# DAE solver settings
##############################
error_bound = 1e-6   # relative accepted error
dt_0 = 1e-4          # initial time step size
end_time = 50        # final integration time

# choose how to compute the initial conditions
INITIAL_CONDITIONS FROM_VARIABLES

# stop the integration if certain variables get out of
# the [0:1] interval -> unstable condition
done = { greater(N_sub, N_pch) + greater(m, 1) + greater(lambda, 1)
         + less(u_i, 0) + greater(u_i, 1) }


##############################
# steady state values
##############################
u_i_star = N_sub/N_pch
lambda_star = N_sub/N_pch
m_star = lambda_star + (log(1+N_pch*(1-lambda_star)))/N_pch
rho_e_star = 1/(1 + N_pch*(1-lambda_star))
u_e_star = u_i_star + N_sub*(1-lambda_star)
eta_star = 1

##############################
# initial conditions
##############################
l_1_0 = lambda_star * 1/N_1
l_2_0 = lambda_star * 2/N_1
l_3_0 = lambda_star * 3/N_1
l_4_0 = lambda_star * 4/N_1
l_5_0 = lambda_star * 5/N_1
l_6_0 = lambda_star * 6/N_1
m_0 = m_star
u_i_0 = u_i_star*0.9
u_e_0 = u_e_star
rho_e_0 = rho_e_star
eta_0 = eta_star

##############################
# the dynamical system equations
##############################
# equations (29)
DAE 0.5*(      0 + l_1_dot) + N_1*(l_1 -   0) - u_i
DAE 0.5*(l_1_dot + l_2_dot) + N_1*(l_2 - l_1) - u_i
DAE 0.5*(l_2_dot + l_3_dot) + N_1*(l_3 - l_2) - u_i
DAE 0.5*(l_3_dot + l_4_dot) + N_1*(l_4 - l_3) - u_i
DAE 0.5*(l_4_dot + l_5_dot) + N_1*(l_5 - l_4) - u_i
```

```
DAE 0.5*(l_5_dot + l_6_dot) + N_1*(l_6 - l_5) - u_i

# equation (31)
DAE u_i - u_e + N_sub*(1-lambda)

# equation (34)
DAE rho_e - 1/(1+eta*N_pch*(1-lambda))

# equation (35)
DAE lambda - m + log(1/rho_e)/(eta*N_pch)

# equation (36)
DAE m_dot + rho_e*u_e - u_i

# equation (30)
DAE  {
   + m*u_i_dot + m_dot*u_i - N_sub*(1-m)/(eta^2*N_pch)*eta_dot - N_sub/(eta*N_pch)*m_dot
   + rho_e * u_e^2 - u_i^2
   + m/Fr - Eu
   + k_i*u_i^2 + k_e*rho_e*u_e^2
   + Lambda*( m*u_i^2
              + (N_sub*log(1/rho_e))/(eta*N_pch)^2*(N_sub/(eta*N_pch) - 2*u_i)
              + lambda^2*N_sub^2/(2*N_pch)
              + 2*u_i*N_sub*(1-lambda)/(eta*N_pch)
              + N_sub^2/(eta*N_pch)*((0.5-lambda)-(1-lambda)/(eta*N_pch))
            ) }

##############################
# output results
##############################
FILE output channel-eta.out

PRINT FILE output HEADER TEXT "\#␣vertical␣boiling␣channel"
PRINT FILE output HEADER N_pch  TEXT "\#␣N_pch␣=␣"
PRINT FILE output HEADER N_sub  TEXT "\#␣N_sub␣=␣"
PRINT FILE output HEADER Fr     TEXT "\#␣Fr␣=␣"
PRINT FILE output HEADER Lambda TEXT "\#␣Lambda␣=␣"
PRINT FILE output HEADER k_i    TEXT "\#␣k_i␣=␣"
PRINT FILE output HEADER k_e    TEXT "\#␣k_e␣=␣"
PRINT FILE output HEADER Eu     TEXT "\#␣Eu␣=␣"

# print phase portrait both in stdout and in channel-eta.out
PRINT t lambda u_i m   FILE output
PRINT t lambda u_i
```

A similar file can be constructed for the original Clausse and Lahey model (42). Parametric studies (e.g. figure 8) can be done with little effort by using the `PARAMETRIC` keyword. See http://ib.cnea.gov.ar/~thelerg/channel.php for further and updated information about the model and related analysis software.